Donor bound-exciton excited states in zinc selenide

P. J. Dean and D. C. Herbert
Royal Signals and Radar Establishment, Malvern, Worcs, England

C. J. Werkhoven, B. J. Fitzpatrick, and R. N. Bhargava
Philips Laboratories, Briarcliff Manor, New York

(Received 8 August 1980)

Accurate measurements of donors in selective photoluminescence (SPL) and photoluminescence excitation (PLE) spectra have been made with a tunable dye laser for relatively pure vapor and solution-grown single crystals of ZnSe. The donor species are identified by reference to the work of Merz *et al*. Very accurate agreement is found for the $1s$-$2s,p$ excitation energies, though not for the absolute photon energies. A new bound exciton (BE) falling just above the donor BE is shown *not* to involve a further donor species. Improved values are derived for effective-mass donor binding energy, the electron effective mass, static dielectric constant, internal binding energy of the free exciton (FE), and the free-particle band gap in ZnSe. Large differences in the PLE spectra of excitons bound to ionized compared with neutral donors, as well as for neutral acceptors and other BE, are attributed to the dominance of free electron-hole pairs in the excitation channel for the former and FE for the latter luminescence. Landau-level effects appear in the PLE for ionized donor luminescence. New excited BE states appearing just below the $n = 2$ FE energies are shown by SPL to involve *neutral* donors. Their wave-function character is contrasted with the donor bound-exciton excited states just below the $n = 1$ FE. The nature of splittings observed in ionized donor BE is discussed.

I. INTRODUCTION

Donors contribute to the near gap (edge) luminescence of semiconductors in a variety of ways. The resulting transitions are very useful for the characterization of chemical species and are also of considerable interest for the information they provide on the donor states and on the properties of the host semiconductor. We are concerned in this paper not with the interimpurity, donor-acceptor pair transitions which constitute the true "edge luminescence" first defined in a direct-gap II-VI semiconductor,[1] but rather with the sharp low-temperature luminescence and absorption lines and their satellites lying even closer to the semiconductor band gap and which involve bound excitons. The donor bound excitons (DBE) are present in two forms, the I_2 lines which involve excitons bound to *neutral* donors and the I_3 lines, where the binding is to *ionized* donors. The I_1 lines involve excitons bound to neutral acceptors according to the nomenclature of Thomas and Hopfield assigned initially in CdS.[2] Numerous theoretical papers discuss BE stability at these impurity centers.[3] However, an early prediction[4] that stable I_3 lines can exist only for low values of the electron to free-hole effective-mass ratio, $\sigma = m_e^*/m_h^*$, such as occurs for direct-gap semiconductors like ZnSe, remains qualitatively correct. The analogous species involving ionized acceptors then cannot form bound states. Both types of DBE complexes have been identified for a number of donor species in ZnSe by Merz *et al*.[5] in a paper hereafter designated MKNS. These authors have also reported the existence of four excited states of the I_2-like DBE and the "two-electron" satellite transitions associated with several of these states, together with the lowest "principal" DBE state. These "two-electron" satellites involve BE recombinations which leave the neutral donor in one of a series of possible excited orbital states, principally $2p$ and $2s$. MKNS observed the splitting of the $2p$ final states in a magnetic field and derived some parameters of the free electron and of the effective-mass (EM) donor in ZnSe. They also noted a single excited state of each I_3 DBE and reported on their variation with chemical species. No conclusions were reached about the nature of the excited DBE states for the I_2- or I_3-like luminescence lines.

In the present paper, we exploit the advantages of tunable dye laser excitation to obtain detailed photoluminescence excitation (PLE) and selective photoluminescence (SPL) spectra involving both types of DBE and, for comparison, the principal acceptor bound excitons (ABE). In the PLE technique the intensity of an emission is monitored while the exciting light source is energy scanned. This mode of excitation allows one to isolate absorption processes preferentially for a given luminescent transition. In SPL, photoluminescence spectra are recorded using different wavelengths for excitation. This process allows one to resonantly excite certain luminescent transitions and separate the contributions from other overlapping luminescent bands. The advantages of these techniques

are becoming well known.[6,7] These are mainly that the PLE spectra can be obtained with resolution ~0.1 meV (~1 cm^{-1}) adequate to ensure that only single narrow satellite or principal BE components are detected, giving the strongest possible isolation from extraneous excitation processes. Complementary advantages occur in SPL.[7] Using this technique, we confirm the $1s$-$2p$ and $1s$-$2s$ excitation energies reported by MKNS and observed by us for several donor species in a number of ZnSe crystals, both solution and vapor grown. However, we find absolute photon energies upshifted by ~0.25 meV compared with MKNS (Sec. III B). Selective excitation by the narrow line from the tunable dye laser removes much of the inhomogenous broadening from the principal DBE lines and their satellites. Consequently, we observe "two-electron" transitions to $n=3$ orbital states more clearly and obtain improved values of the effective-mass donor binding energy D_D^{EM} and the central-cell corrections to donor ground-state energies E_D (Sec. III B). Higher DBE excited states than those reported by MKNS are also observed (Sec. III B). Magnetic splittings of transitions to $2p$ donor states yield the electron effective mass m_e^* and spin-splitting parameter g_e (Sec. III C). Resonant excitation into the major donor excited states confirm that these involve p-like BE wave functions. This confirms their identification with p-like orbital excited states of the bound hole[8] as concluded very recently for similar transitions in ZnTe.[9,10] A major new result in this paper concerns extrinsic features of the PLE spectra just below the $n=2$ free exciton (FE) energy of ZnSe (Sec. III F). Sharp two-electron satellites characteristic of the principal donor species are observed in SPL spectra for these excitation components, confirming their identification with neutral DBE excited states. It is argued that these states involve excitations within the weakly bound exciton, whereas the lower-lying DBE excited states observed just below the $n=1$ FE involve excitations of the BE relative to the neutral donor. One of these high DBE-excited components, falling particularly close to the $n=2$ FE, contains BE states with an even more s-like character than the principal DBE, whereas a second component contains BE states with dominant p-like character. Excitations involving different donors and different states of a given donor both contribute to the broad higher-energy excitation feature. Minima in excitation spectra of all BE components mark the $n=1\rightarrow 3$ components of the FE, from which significantly revised values of the exciton binding energy E_X and free-particle band gap E_G are derived (Sec. III E). Dramatic differences occur between PLE spectra of I_3 DBE components and all other I_2 DBE and I_1 ABE luminescence components examined (Sec. III D). The major excitation channel for I_3 luminescence involves the creation of free electron-hole pairs, whereas FE creation is much more important for the excitation of all other BE, including an unknown BE I_α of small localization energy E_{BX} which may involve an isoelectronic molecular complex (Sec. III A). Landau-level effects are observed in the strong excitation feature for I_3 luminescence occurring just above E_G at zero magnetic field (Sec. III D). Very different relative strengths of excitation series at energies well above E_G, involving the cascade emission of LO phonons, are noted in PLE spectra of luminescence at different types of BE centers (Sec. III D).

II. EXPERIMENTAL

The single crystals used in the present work were grown by liquid phase epitaxy (LPE) from Sn or Bi solutions, slowly cooled from below 950 °C in a covered purified graphite multi-well boat of the type used for crystal growth of III-V semiconductor devices.[11] This work has established that major problems of contamination exist by impurity out-diffusion from the single-crystal substrates during growth.[12] Strenuous attempts were made to reduce this problem by appropriate substrate-cleaning procedures before growth, including soaking in molten metals. These treatments have resulted in a noticeable reduction in the tendency to compensation of acceptor dopants,[12] though they have not yet provided fluent p-type conductivity. The quality of their near-band-gap photoluminescence spectra approaches the best freely nucleated single crystals grown from the vapor by a sublimation process near 1050 °C.[13] The best spectra were obtained from double LPE crystals, wherein the properties of the second layer of typical thickness ~6 μm were improved through the isolation of some of the deleterious influences originating in the substrate by growth of an initial LPE layer of thickness ~4 μm. Probably, the dilution effects of a first liquid-Sn source play a significant role in the reduction of the background doping level and the corresponding increase in spectral quality to the level reported in this paper, with linewidths of principal DBE lines of ~0.19 meV, about half that of typical single LPE material and comparable with the best vapor-grown crystals. These LPE layers have great advantages of homogeneity of morphology and electronic properties compared with the vapor-grown crystals, which are often twinned and intergrown with only small single-crystal regions. A few vapor-grown crystals of high optical quality,

including some of those used by MKNS in pioneering work on the identification of donor species in ZnSe, were available for cross-checking optical data from the LPE material.

The optical spectra were recorded with the samples freely suspended in liquid He, usually at 4.2 K. Excitation by ~50-mW 441.6-nm light from a He-Cd laser was very useful for survey work, although 413.1-nm and ~360-nm light from a Kr^+ laser was also used. Although the excitation efficiency was appreciably lower, the advantage of the shorter-wavelength excitation was that the exciting light could be efficiently removed by a suitable dye filter, for example, Wratten No. 2*E*, placed before the entrance slit of the $f/17$ 2*m* Baird Atomic spectrometer. This filtering was essential for recording pure luminescence spectra from some of the less efficient samples. The 441.6-nm light falls only very slightly above the $n=1$ free-exciton state of ZnSe, and provides efficient luminescence excitation relatively free of most problems of surface recombination.

Spectra were recorded photographically from all samples both for survey purposes and because this technique is the most sensitive for the recognition of poorly resolved small splittings in the zero-field spectra, for example, the ~0.2-meV splitting of the I_I^{DEEP} BE and those of the magnetic subcomponents at the modest magnetic fields necessary to ensure that states from adjacent zero-field components overlap to a minimum degree. However, most of the data reported in this paper were obtained photoelectrically, using a scanning attachment at the focal plane of the spectrograph. The laser light was chopped at ~325 Hz and the sample luminescence detected synchronously using a lock-in amplifier. Luminescence spectra were recorded using an HP 9825 calculator-controlled system with a remote video data display unit, arranged so that spectra corrected to constant energy dispersion were available at the calculator printer. Facilities for line calibration, data expansion, differentiation, and smoothing were built in to the calculator program.

Most of the spectra reported in this paper involve SPL or are PLE spectra obtained with a Coherent Radiation Model 590 dye laser pumped by ~2 W of ~360-nm light from a Coherent Radiation Model 3000 K Kr^+ laser. The dye used was Stilbene III, which provided an output of ~50 mW after the chopper over the relevant spectral range of these measurements, between ~2.78 and ~2.9 eV. The effects on the PLE spectra of occasional sudden jumps in dye laser output intensity and of the slowly varying change in output over this range of photon energy were recognized from comparative measurements with a ratiometer. The denominator channel of the ratiometer was fed from an Si photodiode, which received light reflected from the back of the chopper at the dye laser output. The signal-to-noise ratio was degraded significantly through use of the ratiometer, so most of the PLE spectra reported here were taken from the essentially noise-free data obtained directly from the output of the lock-in amplifier. The spectral parameter was the angle of the Lyot tuning filter of the dye laser, which was altered by a micrometer screw driven by a stepping motor. The relationship between the setting of this screw and the output wavelength or photon energy was obtained empirically and is a smoothly varying, slightly superlinear function above 2.78 eV. These PLE spectra are not corrected to constant energy dispersion.

III. RESULTS AND DISCUSSION

A. No-phonon line near 2.7982 eV

A significant initial motivation for this study was the line I_α^0 first observed by Werkhoven *et al.*[14] near the high-energy limit of the group of principal DBE no-phonon lines which fall just above 2.797 eV in ZnSe. These PL lines involve the shallow donors of greatest significance in promoting *n*-type conductivity in ZnSe. The chemical origin of many lines has been carefully established by MKNS in their work on judiciously back-doped vapor-grown (VG) ZnSe. A typical spectrum of refined LPE ZnSe, shown in Fig. 1(c), contains a triplet structure in the DBE region. The lowest members of this triplet involve the principal DBE transitions of donor species due to In_{Zn} and Al_{Zn} for the particular crystal in Fig. 1, giving the lines I_{20}^{In} and I_{20}^{Al} in the notation of MKNS. The upper member falls close to the DBE excited states I_{2a}^{In} and I_{2a}^{Al}, but not precisely so. The existence of this component as an independent BE is proved by the wide variation in intensity it exhibits relative to the recognized DBE lines between spectra recorded under standard conditions from different crystals, varying between cases where I_α^0 was ~10 times stronger than the strongest DBE line, to cases where it is entirely absent, as in the VG crystals of MKNS. The generic identification of the DBE lines is best proved (Sec. III B) from their associated satellites due to two-electron transitions, shown as I_{2s}^{In}, I_{2s}^{Al}, I_{2p}^{In} in Fig. 1(a) and 1(b). Although we find photoluminesce (PL) line energies uniformly 0.2_5 meV higher than those of MKNS for DBE and ABE transitions (Table I), our results on the two-electron displacement energies below the principal DBE generally agree with MKNS to ± 0.03 meV. These displacement energies are particularly important for donor identifications

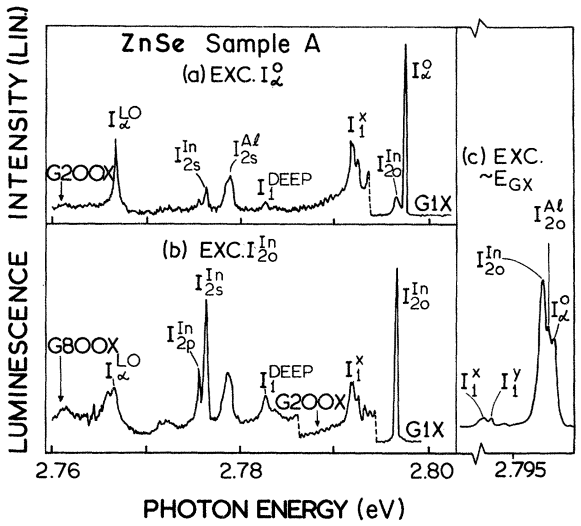

FIG. 1. Photoluminescence spectra from an LPE single-crystal layer of ZnSe 496*H*1 grown from Sn solution (sample *A*) recorded photoelectrically at 4.2 K. Part (c) shows the BE no-phonon components for excitation with the He-Cd laser while parts (a) and (b) are SPL spectra for resonant excitation into unidentified BE components I_α^0 and the donor BE I_{20}^{In}, respectively. Note the much stronger LO-phonon coupling for the α BE. *G* denotes the relative electronic gain, I_1^{DEEP} and I_1^x are acceptor BE's due to Cu and Li, and the remaining nomenclature is described in the text, following MKNS. The LO-phonon energy is 31.8 ± 0.05 meV.

(Sec. III B).

The most obvious possibility is that I_α^0 represents BE PL at some donor not very relevant in VG ZnSe, and relatively shallow according to the spectral position if Haynes' rule applies in ZnSe, as has been established by MKNS for all five donors identified so far. Several properties are inconsistent with this assignment, which can be firmly rejected from their combination. The most striking feature is the strong LO-phonon coupling for I_α^0, Fig. 1(a), $I_\alpha^{LO}/I_\alpha^0 \sim 0.04$, about 100 times larger than for even a relatively deep DBE such as I_{20}^{In}, Fig. 1(b). Phonon coupling is expected to *decrease* with decrease in exciton localization energy E_{BX} (Table I), and there is no obvious explanation for the large increase actually observed. Another inconsistency is the form of the PLE spectrum of I_α^{LO}, which differs significantly from that of a DBE satellite such as I_{2s}^{In} or I_{2s}^{Cl} (Fig. 2), with less contribution from the DBE excited states such as I_{2b}, I_{2d}, I_{20}^*, and $I_{2c,d}^*$, where donor species energy differences are expected and observed (MKNS) to be minimal, and a much larger contribution from free-exciton creation just above $E_{GX}^{n=1}$. The clinching evidence is the complete absence for all crystals of *additional* two-electron satellites in SPL recorded with the laser line tuned to I_α^0, even though the linewidths of such satellites are dominated by the laser line at only ~0.09 meV in many samples, giving excellent conditions for the detection of new lines. This observation, together with the absence of additional DBE excited states in the PLE of I_α^{LO} luminescence, provides conclusive evidence that I_α^0 is not a DBE. Most probably, it involves an exciton bound to a center containing no additional electronic particles, some form of isoelectronic center, point defect, or associate to be discussed elsewhere.[15]

B. "Two-electron" satellites under resonant excitation

As mentioned in Sec. I, the DBE PL spectra and their "two-electron" satellites are rather complex in ZnSe because of the existence of many DBE excited states, each with its own set of satellites and also a result of the common incidence of two or three donor species at comparable concentrations in undoped crystals. It is difficult to backdope to obtain predominance of a selected donor, while preserving crystal quality adequate for detailed spectroscopic analysis. The SPL possible with a dye laser greatly assists in this aim, since a large proportion of the excess spectral linewidth, due to inhomogeneous broadening processes, can be removed under selective narrow-line excitation. This is shown very clearly in Fig. 3, where the principal BE triplet in this case due to In and Al donors and the unidentified α center (Sec. III A) are rather poorly resolved for nonresonant excitation into the very high DBE excited state L_f^0 (Table I), lower right in Fig. 3. Extensive exciton diffusion between spatially inequivalent sites clearly occurs between the absorption event in the very high DBE excited state, $E_{BX} = 0.9_5$ meV, and emission from the lower (principal) DBE state in this case. The spectra (*a*)–(*f*) in Fig. 3 have been arranged to emphasize satellites with constant displacement energies below the laser line due to two-electron transitions. These are enhanced as the laser energy is brought into coincidence, in their turn, with the various DBE excited states listed in Table I. These spectra clearly show a strong increase in the intensity ratio of two-electron transitions to 2*p* and 2*s* donor states as the excitation is tuned from the principal DBE states, subscript *o* [spectra (*a*) and (*b*)], to the DBE excited states, subscript *a*, *b*, *d*, etc. [spectra (*c*), (*d*), and (*e*)]. Such an increase has been observed in resonantly excited DBE luminescence in ZnTe (Refs. 9, 10) and interpreted in favor of an earlier theoretical model in which the main DBE excited components are described by excitations of the

TABLE I. Transition and localization energies of various principal and excited BE no-phonon components in zinc selenide.

Component	Transition energy (eV)	Localization energy[a] (meV)	Component	Transition energy (eV)	Localization energy[a] (meV)
I_1^{DEEP}	2.7829_3	19.7_7			
	2.7831_4	19.5_6	I_{2a}^{Ga}	2.7982_3	4.4_7
I_1^{Li}	2.7921_9	10.5_1	I_{2b}^{Ga}	2.8002_4	2.4_6
I_1^{Na}	2.7930_6	9.6_4	I_{2c}^{Ga}	2.8012_3	1.4_7
I_3^{In}	2.7941_3	8.5_7			
	2.7945_2	8.1_8	I_{2d}^{Ga}	2.8015_1	1.1_9
I_3^{Cl}	2.7959_8	6.7_2	I_{2a}^{Al}	2.7983_9	4.3_1
	2.7963_8	6.3_2			
	2.7965_5	6.1_5	I_{2b}^{Al}	2.8002_1	2.4_9
			I_{2c}^{Al}	2.8011_1	1.5_9
			I_{2d}^{Al}	2.8013_8	1.3_2
I_{20}^{F}	2.7970_5	6.1_4	$I_{2e}^{Al,In}$	2.8017_2	0.9_8
I_{20}^{In}	2.7972_2	5.4_8	I_{2a}^{Cl}	2.7983_6	4.3_4
I_{20}^{Ga}	2.7975_1	5.1_9	I_{2b}^{Cl}	2.8002_3	2.4_7
I_{20}^{Cl}	2.7977_0	5.0_0	I_{2a}^{In}	2.7980_5	4.6_5
I_{20}^{Al}	2.7977_6	4.9_4	I_{2b}^{In}	2.8001_0	2.6_0
I_{α}^{0}	2.7982_1	4.4_9	I_{2d}^{In}	2.8014_0	1.3_0
			I_{20}^{*}	2.814_2	2.8_0[b]
			$I_{2c,d}^{*}$	2.816_7	0.3_0[b]

[a]Calculated with $E_{GX}^{n=1}=2.8027$ eV, consistent with the low-energy threshold of the LO-phonon-assisted FE band just above 2.77 eV in Fig. 1(b) and with the value from reflectivity, Venghaus (Ref. 25).

[b]Calculated with $E_{GX}^{n=2}=2.817_0$, see Sec. III E in text.

bound hole to a variety of states of p-like character.[8] The slight displacement of peaks from the laser satellite lines marked L^{In} $2p, 2s$ in Fig. 3(b) indicates that these particular luminescence satellites originate from the nonresonantly excited principal DBE state I_{20}^{In}. There is no DBE excited state of the In donor near L_b^0, tuned to I_{20}^{Al} (Table I). Exciton diffusion between donor sites is again responsible for the appearance of BE luminescence from the In donor in this spectrum.

Laser satellite line $L^?$ in Fig. 3(f), displacement energy 17.3_0 meV, is an artifact of the grating, as are the close-in "ghost" lines G in the lower right spectrum. The energy displacements of the sharp lines due to two-electron transitions are given in Table II. The remaining "constant-deviation" line arises from Stokes LO phonon-assisted recombinations of the resonantly excited BE states. The generally broader shifting lines are due to BE recombinations at independent centers. This is clear from Fig. 4 in which the same spectra are presented on a scale of absolute photon energies, rather than energies referred to the exciting laser line. The no-phonon line I_1^{DEEP} is a BE which may involve the deep Cu acceptor.[12,16] The exceptionally strong LO-phonon replica of the I_{α}^{0} BE is again clearly evident in Figs. 3 and 4. Two-electron transitions to the $n=3$ orbital excited state of the donor appear more clearly in Fig. 5, taken from a high-quality VG crystal in which the Ga donor is predominant (Table II) with minor contributions from In and the donor species tentatively identified with F by MKNS. According to Table II, the binding-energy difference between $2p$ and $3p$ donor states is $3.6_2 \pm 0.02$ meV, which implies that the effective-mass donor binding energy E_0 is $26.0_6 \pm 0.15$ meV. This value is significantly smaller than the much less accurate value reported by MKNS, $E_0 = 28.8 \pm 2.4$ meV, but is much more realistic compared with the energies we derive for the donor species (Table II). These also differ significantly from the MKNS values, since our

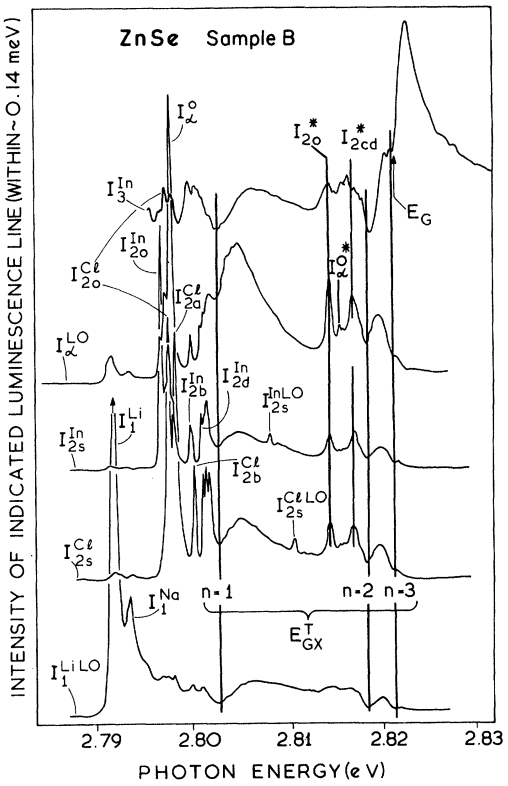

FIG. 2. Comparative low-temperature photoluminescence excitation (PLE) spectra from an LPE ZnSe crystal, 632*H*1 grown from Sn solution (sample *B*) of exceptional purity. The detected luminescence components are noted at the left. The electron-hole band gap is denoted by E_G, while the transverse free exciton gap E_{GX}^T is indicated for various internal excited states of the FE. The notation otherwise is as in Fig. 1, except that excited BE states associated with the $n=2$ FE are denoted by superscript $*$. Lower DBE excited states carry subscripts a, b, and d to differentiate them from the lowest DBE states, subscripts 0.

revised value for the binding energy of the $2p$ state, which must be added to the $1s$-$2p$ donor excitation energies in order to obtaine E_D, is significantly smaller. If we use the electron effective mass m_e^* obtained from the magneto-optical measurements (Sec. III C), we can calculate the low-temperature static dielectric constant using the relationship

$$E_0=\left(\frac{m_e}{\epsilon_s^2}\right)E_h, \tag{1}$$

where E_h is the binding energy of the hydrogen atom. We obtain $\epsilon_s=9.1_4\pm0.1$ if $E_0=26.0_6$ meV and $m_e^*=0.160\pm0.002m_0$, where m_0 is the free-electron mass. This is significantly larger than the unpublished results of Roberts and Marple cited by MKNS, $\epsilon_s=8.66$.

The improved spectral quality of VG crystal sample *C* in Fig. 5 is believed due to a lower total doping concentration compared with the LPE crystal, sample *A*. The intensity of the shallow acceptor-pair luminescence is significantly greater relative to the BE luminescence for crystal sample *C*, with more contribution from Na as well as Li acceptors. The decrease in inhomogeneous broadening associated with this lower concentration is particularly significant for the appearance of the principal DBE under nonresonant excitation and for the spectral quality under excitation into high DBE excited states, particularly the satellites due to recombinations to the $n=3$ donor excited state (cf. Figs. 4 and 5). The identification of the weak satellite labeled I_{20}^{Ga} $3p$ in Fig. 5 was supported by its rapid broadening in a magnetic field resulting from the effects discussed in Sec. III C. The energy shift between the $3p$ and $3s$ states of the Ga donor is ~0.2 meV according to Table II, appreciably smaller than between $2p$ and $2s$, 0.5_0 meV (Fig. 5), or 0.5_4 meV from MKNS. This splitting is dominated by the central-cell effect on the binding energy of even-parity donor states, but decreases with orbital quantum number n appreciably slower than the simple relationship $1/n^3$ predicted from effective-mass theory. This deviation possibly results from an increasing relative contribution from polaron effects for the higher orbital excited states.

C. Zeeman splittings of two-electron satellites

The behavior of the two-electron satellites in a magnetic field was best studied under resonant excitation into one of the DBE excited states, to favor transitions to p-like donor excited states (Sec. III B). These states exhibit a large linear Zeeman effect originating in the orbital magnetism of the p state. Their splittings are observed uncomplicated by the anisotropic spin splittings of the hole in the BE because of the special feature of the resonant coupling of the laser line and the transition to the $1s$ state of the donor.[10] The splitting $\Delta E=\hbar\omega_c$ of the outer components of the Zeeman triplet originating from transitions to the $2p$ donor state in a magnetic field. Fig. 6, lower is given by

$$\Delta E=\hbar eB/m_e^*c, \tag{2}$$

where e is the electronic charge, c the velocity of light, and $\hbar$ is Planck's constant. We obtain an accurate value of m_e^* from this splitting, given in the upper part of Fig. 6.

Each orbital subcomponent exhibits further small splittings into a triplet, as shown in Fig. 6 and with better resolution in the photographic data of Fig. 7. Similar splittings have been ob-

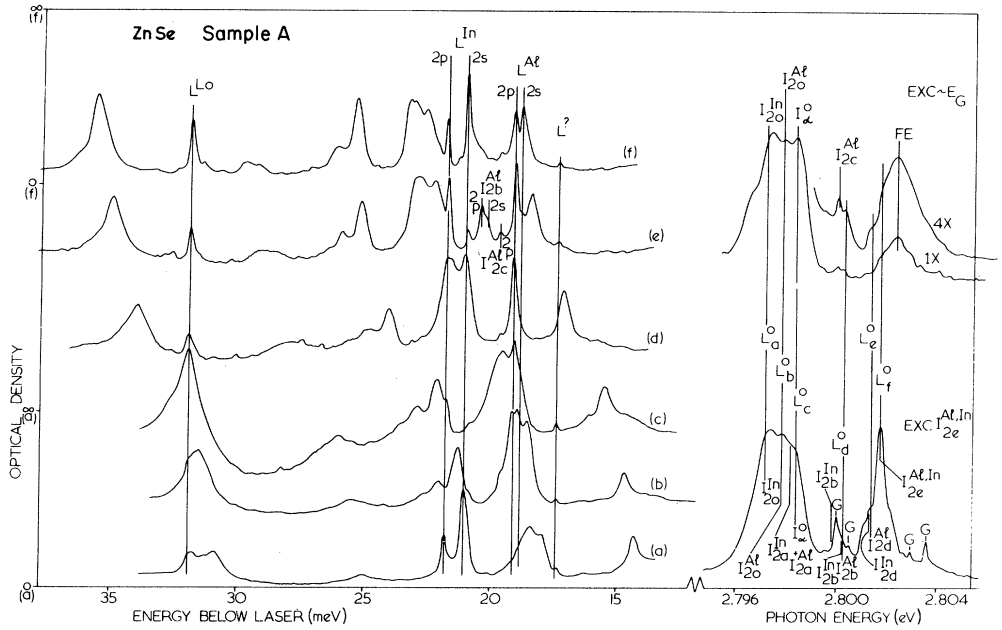

FIG. 3. To the right the low-temperature photoluminescence spectrum recorded photographically in the FE and principal D and α BE region for the crystal used for Fig. 1 (sample A) under excitation near E_G (upper) and within the very high DBE excited state $I^{Al,In}_{2e}$, laser position L^0_f (lower). The laser positions used for spectra $(a)-(f)$ shown at left are indicated through the spectrum at lower right. Spectra $(a)-(f)$ are presented in terms of photon-energy displacement below the laser line. Vertical lines emphasize components of constant displacement energy, due to the indicated "two-electron" satellites of the indicated DBE states and the LO-phonon replica. Components $L^?$ and G are artifacts of the spectrometer.

served for DBE in ZnTe, and identified with spin splittings of the electron in the initial and final states of the transition.[10] Spin-flip processes are possible for the two-electron satellites. We obtain $|g_e| = 1.06 \pm 0.05$ from the measured splittings, in very good agreement with the value obtained from optically detected magnetic resonance in ZnSe, $g_e = +1.13_2$.[17]

The intensity of these resonantly excited satellites of the DBE excited state I^{Ga}_{2b} becomes appreciably weaker above $B \sim 3$ T. A similar phenomenon was noticed in ZnTe for excitation with the fixed-energy 520.8-nm line of the Kr^+ laser, and interpreted as decrease in resonance with the DBE transition caused by diamagnetism.[10] This suggestion was confirmed in the present work. For example, it was found that the satellite intensities of I^{Ga}_{2d} could be substantially restored by $a \sim 0.23$-meV increase in the energy of the dye laser for increase in B from 0 to 3.5 T. This increase is dominated by the diamagnetism of the DBE excited state for the I^{Ga}_{2d} transition, which has E_{BX} only 1.2_6 meV. It is difficult to predict accurately the diamagnetic shift rate of such a p-like DBE state, but the value given above is of the expected order.

TABLE II. Donor excitation energies obtained from "two-electron" satellites and donor ionization energies in zinc selenide.

Donor	$1s$-$2s$ (meV)	$1s$-$2p$ (meV)	$1s$-$3s$ (meV)	$1s$-$3p$ (meV)	Ionization energy E_D (meV)[b]	Chemical Shift (meV)[a]
Al	18.8_4	19.1_2			25.6_4	-0.42 ± 0.16
Cl	19.3_6	19.6_7			26.1_9	-0.13 ± 0.16
Ga	20.1_8	20.7_1	24.1_3	24.3_3	27.2_3	$+1.17 \pm 0.16$
In	20.9_1	21.6_8	25.0_3	25.3_2	28.2_0	$+2.14 \pm 0.16$
F		22.3			28.8	$+2.74 \pm 0.16$

[a] Calculated with effective-mass binding energy $E_0 = 26.0_6 \pm 0.15$ meV.
[b] Calculated with binding energy of $2p$ state $= \frac{1}{4}E_0 = 6.5_2 \pm 0.04$ meV.

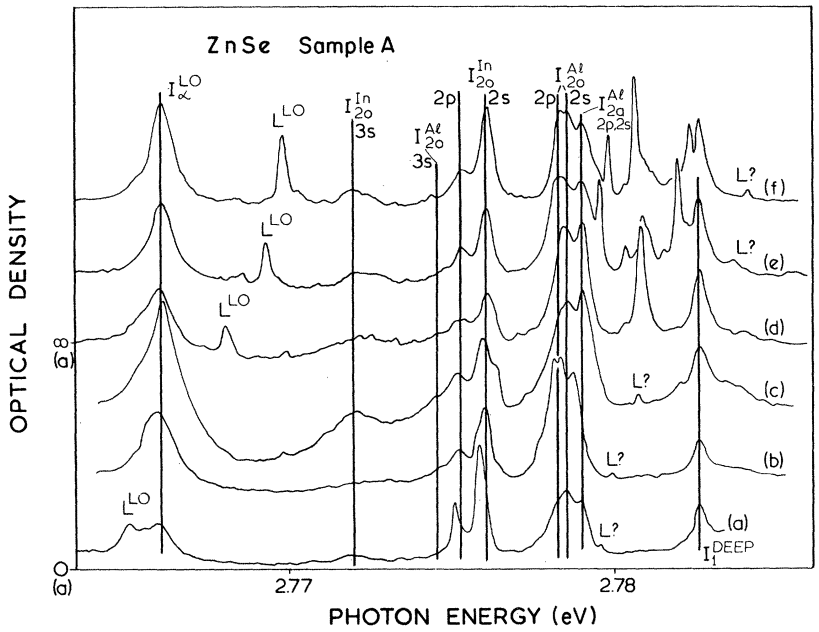

FIG. 4. Contains the data from Fig. 3 (left), represented on a scale of absolute photon energy. Vertical lines emphasize "two-electron" replicas of the indicated DBE components, nonresonantly excited. The large strength of LO-phonon coupling to the α BE is clearly shown relative to the DBE. The notation differs slightly from Fig. 1. For example, a "two-electron" component shown here as I^{In}_{202S} is written simply as I^{In}_{2S} in Fig. 1. The first-level subscript 2 in the former denoted an I_2 (DBE) transition, while that in the latter denotes the $n=2$ orbital state in which the electron is left after recombination occurs, like the second-level subscript 2 in the former.

D. Comparative photoluminescence excitation spectra for different bound-exciton components

We have already noted in Sec. III A the strong differences in PLE spectra of satellites of the DBE and of the unidentified BE line I^0_α. No dramatic differences occur for PLE spectra recorded for detection of I^{In}_{2p} compared with the spectrum for I^{In}_{2s} shown in Fig. 2, as expected. Although the different donor-related BE excited-state excitation features shown in Fig. 2 involve electron and hole wave functions of quite different parity, including components I^*_{20} and $I^*_{2c,d}$ (Sec. III F), their contribution to the PLE of I^{In}_{2s}, I^{In}_{2p} involves an intermediate step of nonconservative energy relaxation to the DBE ground state I^{In}_{20} before luminescence occurs. The intensity ratio of transitions to I^{In}_{2s} and I^{In}_{2p} is determined by the properties of the I^{In}_{20} DBE state. Differences between the PLE spectra for the In donor satellites and that for I^{Cl}_{2s} in Fig. 2, besides the anticipated differences in the principle DBE features, can be ascribed to small differences in the energies of the DBE excited states, for example I_{2a}, I_{2b}, between these two donors as already reported by MKNS. Excitation into I^{In}_{20} cannot produce I^{Cl}_{2s} luminescence in low-temperature spectra, since I^{In}_{20} lies ~0.5 meV below I^{Cl}_{20}, an energy $>kT$ at 4.2 K (0.36 meV), where kT is the kinetic energy factor.

Much greater differences are observed in PLE spectra for detection of other BE components. For example, the lowest spectrum in Fig. 2 shows that creation of BE at the donors and even at the Na acceptor makes minor contributions to the luminescence of excitons bound at neutral Li_{Zn} acceptors. Clearly nonconservative BE diffusion between donor and acceptor sites is very improbable in such a relatively pure LPE sample at low temperatures. The sharpness of the principal BE lines in this crystal (Fig. 8) shows that these BE, particularly the A BE, are well localized (compared with Figs. 1 and 3).

The most striking differences occur between all the PLE spectra described so far and that of the I^{In}_3 line shown at the top of Fig. 2. This BE component involves BE recombination at an *ionized* donor, a general feature of the near-gap luminescence of direct-gap semiconductors with sufficiently low value of the electron-to-hole effective-mass ratio $\sigma = m^*_e/m^*_h$, and also discussed for ZnSe by MKNS. Once again we obtain very good agreement with MKNS for the energies of the different I_3 lines for these donors only if we

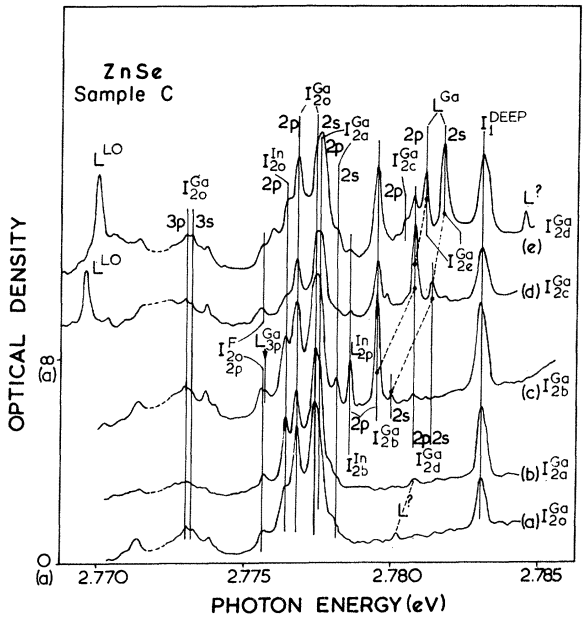

FIG. 5. Low-temperature photoluminescence spectra recorded photographically from a high-quality VG ZnSe single crystal S953 (sample *C*) to show the "two-electron" satellites for excitation in the DBE components indicated to the right, according to the nomenclature of MKNS. A single donor Ga_{Zn} is dominant in this case, unlike Fig. 1. Transitions which leave the donor in the $n = 3$ orbital states can be recognized as well as the strong transitions to the $n = 2$ states. The large intensity changes consequent to selective excitation of the different DBE are even more evident than in Figs. 3 and 4.

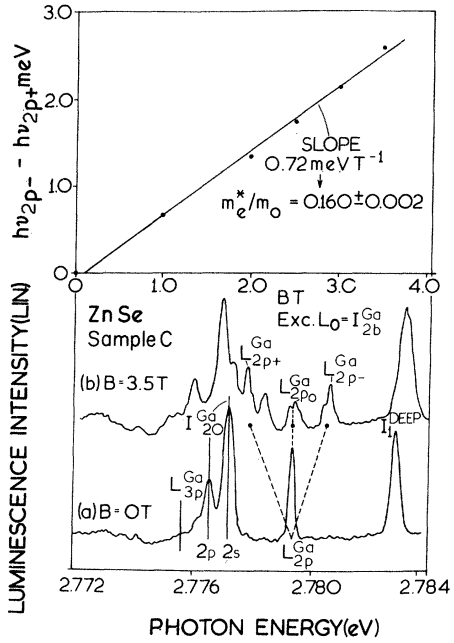

FIG. 6. The lower part shows the effect on the "two-electron" satellites in the ZnSe VG single crystal (sample *C*) of Fig. 5 of a magnetic field of $B = 3.5$ T. The spectra were recorded photoelectrically for selective excitation in the second excited state of the DBE of the Ga donor. The major effect is seen as a splitting of the initially strong, narrow satellite due to recombinations from *this* BE to the $2p$ state of the electron. The three magnetic subcomponents result from a splitting of this orbitally degenerate state as indicated by the subscripts. Further splitting of each subcomponent due to spin can just be seen, but is partially obscured by the instrumental resolution employed. The upper part shows the linear magnetic field dependence of the splitting between the outer groups of magnetic subcomponents, as indicated.

increase all their energies uniformly by 0.24 meV. The relative intensities of the associated weak components at slightly higher photon energy (Table I) are rather appreciably greater in the 4.2-K spectrum at the top of Fig. 8 than in the 1.6-K data of MKNS, as expected. We have not been able to resolve magnetic subcomponents of these I_3 lines up to $B = 3.5$ T. However, we note that two or three zero-field subcomponents are expected from a combination of $J - J$ and crystal-field splitting for a single electron-hole pair bound to a T_d site impurity in ZnSe.[18] We clearly observe three subcomponents for the Cl donor (Table I) but can only speculate that the weak narrow doublet centered ~0.5 meV *above* the strong component (Table I) may be caused by forbidden transitions from the $J = 5$ BE state split by the T_d field of the impurity ion. If this assignment is correct, the $J - J$ splitting is inverted compared with expectation from Hund's rule and the usual configuration.[18] The assignment is supported by the absence of magnetically enhanced lines below the strong I_3^{Cl} (or I_3^{In}) line, which would be expected for normal ordering due to a combination of thermalization and mixing of zero-field BE states in the magnetic field.[18]

The main difference between the PLE spectra of I_3^{In} and the remaining spectra in Fig. 2 is the suppression of all features connected with neutral *D* or *A* BE and the strong enhancement of response above the energy gap near 2.821_5 eV for free electron-hole pair creation in the I_3^{In} spectra. The PLE spectrum of I_3^{Cl} is very similar except for a major difference near $I_{2c,d}^{*}$ unconnected with I_3^{Cl} luminescence, as discussed in Sec. III E. All these spectra contain dips near the energies for free exciton (FE) creation in the states of different orbital quantum number noted in Fig. 2. These features will be discussed further in Sec. III F.

We conclude from the differences in the PLE spectra noted above that the main excitation channel for I_3 BE luminescence does not involve the

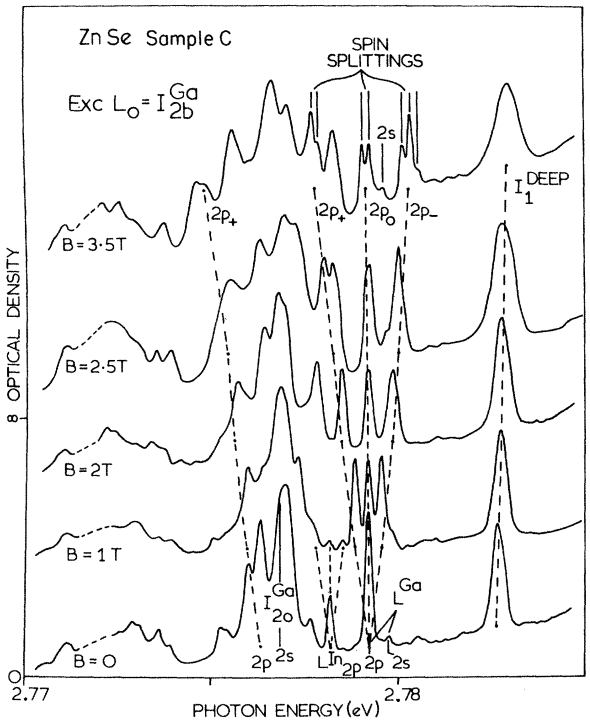

FIG. 7. Zeeman splittings of the low-temperature "two-electron" photoluminescence satellites from the crystal used in Fig. 6 (sample C). These spectra were recorded photographically with higher resolution than in Fig. 6, to reveal the spin substructure much more clearly. Even so, these densitometer recordings do not do justice to the quality of the original photographic data. Similar splittings due to orbital magnetism of the bound electron occur in the satellites from the nonresonantly excited DBE components. However, they are much harder to interpret because of the much greater zero-field width of these no-phonon lines, the greater complication of the Zeeman pattern due to contributions from the hole in the BE, and because two-electron transitions to the $2s$ donor state, which has no orbital magnetism, predominate in recombinations from the lowest DBE state.

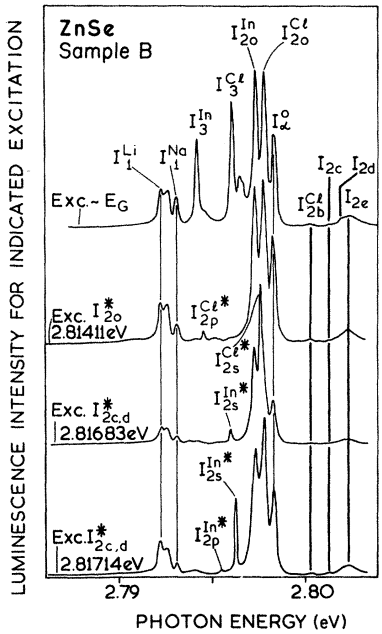

FIG. 8. Low-temperature photoluminescence from the LPE ZnSe single crystal (sample B) used in Fig. 2, recorded photoelectrically for excitation at the positions indicated at the left. These spectra contain only the shallow ABE and DBE components. The excitation is selected to emphasize the I_3 DBE lines in the upper spectrum, but is chosen below to produce optimum strength of the major "two-electron" satellites of the DBE excited-state components. I^*_{20} and $I^*_{2c,d}$ which fall just below the $n=2$ FE (Fig. 2). These satellites are indicated by a superscript $*$. The notation for these two high DBE states was chosen to emphasize that their separation is similar to that between the lower DBE states with corresponding subscripts (Fig. 2), but may have no special significance.

creation of FE or BE, but is sensitive to electron-hole pair production. Donor species in these ZnSe crystals are substantially compensated at equilibrium. However, they have a very large cross section for the capture of free electrons at low temperatures due to their Coulomb-attractive potential which produces many shallow bound states at energies near kT at 4.2 K.[19] A large proportion of donors may be expected to be photoneutralized by direct electron excitation from the valence band at laser energies $h\nu > h\nu_I$, which is also $> E_g - E_D$. Absorption processes which produce FE will then lead to I_2 or I_1 BE luminescence, not I_3. However, free holes are produced at $h\nu > E_G$ and these can form I_3 BE by capture at neutral donors. Thus, the low-energy threshold of the main PLE feature for I_3 luminescence marks the energy gap E_G, while the rapid decrease beyond the peak about 1.5 meV above threshold can be ascribed to the effects of nonradiative recombination of strongly absorbed light at the crystal surface according to the theory of De Vore.[20]

Strong support for the identification of this feature with band-to-band absorption is obtained from Fig. 9(b). The structure observed above the peak, increasing rapidly in visibility and complexity with magnetic field B, is qualitatively consistent with the magneto-optical behavior expected at the band edges. The dominant effect occurs in the conduction band because of the low value of $\sigma = m_e^*/m_h^*$, $\sigma \sim 0.3$ in ZnSe. Several peak separations closely similar to the energy $\hbar\omega_c$ anticipated for the conduction-band Landau-level

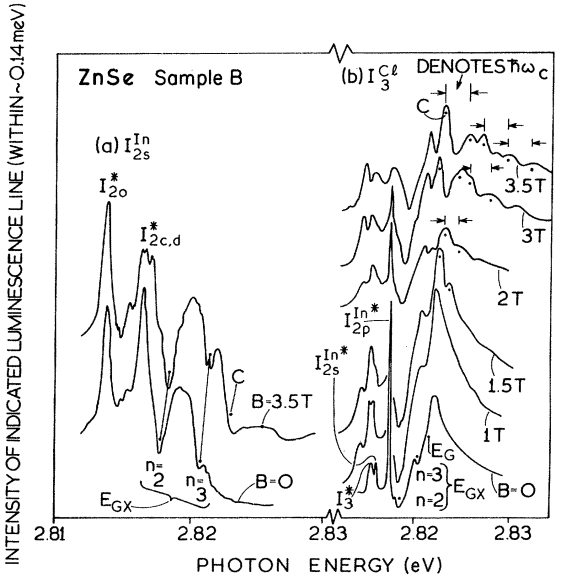

FIG. 9. Part (a) shows detail of the low-temperature PLE spectra of the ZnSe crystal used in Fig. 2 (sample B) for photoelectric detection of the "two-electron" satellite I_{2s}^{In}, at zero magnetic field and $B = 3.5$ T. The high DBE excited states I_{2o}^{*} and, particularly $I_{2c,d}^{*}$ broaden and shift in the magnetic field. Minima marking the $n = 2$ and $n = 3$ states of the FE also show substantial upshift due to diamagnetism. Part (b) is like (a) except that I_3^{Cl} is detected, giving a strong contribution to the PLE from the absorption component commencing at E_G (lower spectrum). This component develops appreciable structure in a magnetic field of ≥ 1.5 T, caused by Landau-level structure in the bands. The energy $\hbar\omega_c$ is the same as the splitting in the upper part of Fig. 6. The very sharp components $I_{2s,2p}^{In*}$ appear in these spectra due to accidental overlap of these "two-electron" satellites with the nominally detected I_3^{Cl} component (see text).

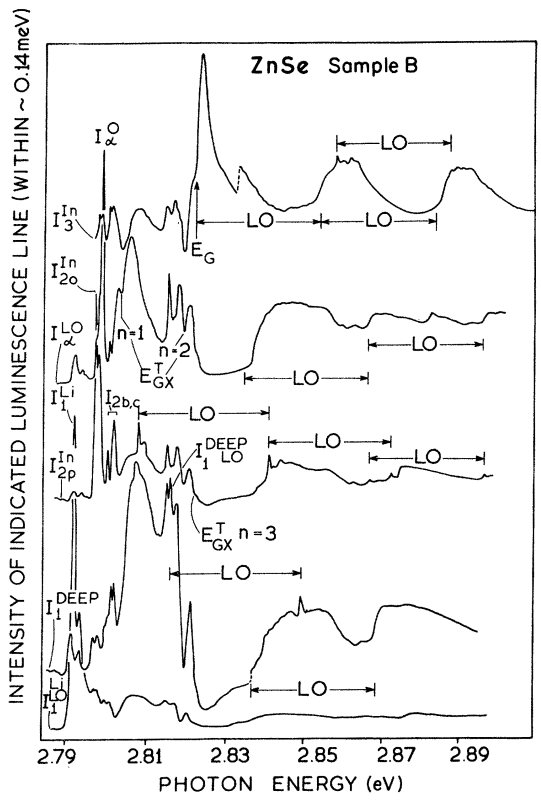

FIG. 10. Contains low-temperature PLE spectra for a slightly different variety of detected photoluminescence components than used in Fig. 2 (sample B), indicated at the left, recorded photoelectrically for the same crystal over a wider range of photon energy. Note that the spectrum for I_3^{In} luminscence is nearly exactly complementary to those for I_{α}^{LO}, I_{2p}^{In}, and I_1^{DEEP} luminescence with regard to contributions from near $E_G + n\hbar\omega_{LO}$, where n is an integer.

structure, identical to those given in the upper part of Fig. 6, can be recognized in these spectra. Account must be taken of the complex magneto-optical behavior of the degenerate valence-band maximum in a detailed interpretation of these spectral oscillations, and this will not be attempted here.

The main features of the PLE spectra of these BE states for energies well above E_G are oscillatory series involving the LO-phonon energy $\hbar\omega_{LO}$ (Fig. 10). These effects are quite well known, and have been observed for several semiconductors.[21,22] When associated with intrinsic absorption features, they originate from the fact that the relaxation time for scattering by LO phonons is much faster than any other energy dissipation process. Thus free electrons, holes, or excitons created high in the bands are returned to an energy within $\hbar\omega_{LO}$ of E_G or E_{GX} before significant scattering by acoustic phonons, or free-particle luminescence or capture into bound states can occur. Energy randomization occurs by scattering between electronic particles to achieve an effective temperature well above that of the lattice at 4.2 K.[23] The main feature of Fig. 10 of particular interest in the present paper is the considerable difference in relative strength of contributions well above E_G between the PLE spectra of different BE components. The strongest occurs for detection of the I_3 luminescence, where the broad components with threshold energies at approximately $E_G + n\hbar\omega_{LO}$ confirm the importance of low-energy free electron-hole pairs in the creation of excitons bound to ionized donors. The sharp lines above 2.855 eV are close to $2\hbar\omega_{LO}$ and $3\hbar\omega_{LO}$ above the detected luminescence line I_3^{In}. The PLE spectra of I_{2p}^{In} and, particularly, I_{α}^{O} and I_1^{DEEP}, contain strong broad structure with threshold energies close to $E_{GX} + n\hbar\omega_{LO}$, confirming the

importance of FE creation for the formation of these BE. This effect is also clear from the strong contributions immediately above the negative features at E_{GX}^{T}, particularly pronounced for I_{α}^{0} and I_{1}^{DEEP} luminescence. The superimposed sharp-line series for I_{2p}^{In} and I_{1}^{DEEP} again occur at $n\hbar\omega_{\mathrm{LO}}$ above the detected luminescence energies. The PLE spectrum of I_{1}^{DEEP} luminescence contains weak dips near the top of many of the extrinsic features such as I_{1}^{Li}, I_{20}^{In} and I_{2c}, showing relatively inefficient energy transfer for BE luminescence at a center with relatively large E_{BX}.

E. Free-exciton energies from PLE spectra

We have seen that the PLE spectra of all detected BE states contain narrow minima near 2.8028, 2.8170, and 2.820_6 eV. The first of these is close to the energy accepted[24] for the transverse FE, E_{GX}^{T} and marked as $n=1$ in Figs. 2, 9, and 10 since it corresponds to the ground state of binding of the relatively light electron in the Coulomb field of the hole. If the second dip marks the $n=2$ FE state, then the excitation energy of 14.2 meV corresponds to $0.773\,R_0^*$ for a valence-band parameter $\mu=0.20$ (Ref. 25), where R_0^* is the Rydberg energy of the FE.[26] Thus, $R_0^*=18.4\pm0.5$ meV is appreciably larger than that reported by Venghaus[25] from magnetoreflectivity $R_0^*=16.8\pm0.4$ meV but smaller than that of Sondergeld and Stafford[27] from the $2p-3p$ FE energy separation measured by two-photon absorption, $R_0^*=19.9$ meV. Thus, according to the analysis of Baldereschi and Lipari,[26] E_{1s} for the FE is 19.0 ± 0.5 meV and $E_G=E_{GX}^{T}+E_{1s}=2.821_8$ eV. This value of E_G is very close to the value obtained from the low-energy threshold of the strong component in the PLE spectrum of I_3 luminescence in Figs. 2, 9, and 10, $2.821_5\pm0.0005$ eV.

Further confirmation of this intermediate value of E_{1s} and E_G is obtained from the identification of the dip near 2.820_6 eV with the $n=3$ state of the FE. This gives a splitting between $n=1$ and $n=3$ of 17.8 meV. The minimum marked $n=2$ and $n=3$ in Fig. 9(a) show substantial diamagnetic shifts between $B=0$ and $B=3.5$ T, respectively, ~0.7 and 0.9 meV, corresponding to shift rates of ~5.6 and $\sim7.3\times10^{-2}$ meV T^{-2}.

F. Extrinsic features in PLE spectra above $n=1$ FE

Two strong peaks appear in the PLE spectra of I_{2s}^{Cl}, I_{2s}^{In}, I_{α}^{LO}, and I_{1}^{DEEP} luminescence in Figs. 2 and 10, shown in more detail for I_{2s}^{In} in Fig. 9(a). Similar peaks have been observed in the optical absorption and DBE PLE spectra in ZnTe.[6] They were not studied in detail, but were attributed to excited DBE states with the $n=2$ state of the FE because of their large diamagnetic shift rates, roughly as expected for the large radius of the electron bound in an $n=2$ orbital state.[28] The centroid of component $I_{2c,d}^{*}$ also show a substantial upshift in energy between $B=0$ and $B=3.5$ T, about 0.5 meV. This corresponds to a diamagnetic shift rate of $\sim4.1\times10^{-2}$ meV T^{-2}, comparable to that reported for the $n=2$ FE in Sec. III E. The exact value is difficult to determine because of the appearance of substructure on the $I_{2c,d}^{*}$ peak which is only partially resolved at $B=3.5$ T [Fig. 9(a)]. The diamagnetic shift rate of component I_{20}^{*} is only ~0.2 meV, corresponding to a shift rate of $\sim1.6\times10^{-2}$ meV T^{-2}. The ratio of these shift rates ~0.4 is roughly in inverse proportion to the ratio of the BE excited-state localization energies measured from the $n=2$ FE,

$$(E_{BX})I_{20}^{*}/(E_{BX})I_{2c,d}^{*}=3.8\ \mathrm{meV}/1.3\ \mathrm{meV}=2.9\,,$$

as expected for a bound state.

Proof of the assignment of these PLE features I_{20}^{*} and $I_{2c,d}^{*}$ to excited states of the DBE is afforded by SPL spectra such as that at the bottom of Fig. 8. Sharp luminescence satellites spaced below the excitation energy by *exactly* the $1s-2s$ and $1s-2p$ excitation energies of the In or Cl donors were observed. Visual observation at the spectrograph focal plane gave dramatic proof that these sharp satellites shifted in energy with the laser line. However, they could be detected readily only over a narrow energy range while the dye laser line remained substantially within the linewidth of the relatively broad excitation band. For example, the sharp replica $I_{2s}^{\mathrm{In}*}$ (Fig. 8, lower) was observed only while the laser energy was translated by $\sim0.4_5$ meV across PLE component $I_{2c,d}^{0}$ shown in Fig. 9(a). These PL satellite components retained essentially the same half-width as the laser line itself, ~0.09 meV. Besides affording dramatic proof that these PLE features are intimately associated with *neutral* donors, these observations also show that the majority of their large linewidths arise from inhomogeneous broadening, whose effect can be removed by the spatial (donor) site selectively afforded by selective optical excitation. Similar dramatic line narrowing in SPL has been observed for the principal DBE components when these are broadened by comparable amounts in doped crystals of ZnTe.[10] Visual observation also showed that excited DBE states belonging to *different* species contribute to the zero-field linewidth of these excited DBE states. Thus, an increase of excitation energy of only 0.31 meV from a value close to the zero-field peak energy of $I_{2c,d}^{*}$ caused a substantial shift from a lumines-

cence spectrum dominated by resonant Cl donor satellites to one dominated by satellites of the In donor, measured relative to the contributions from nonresonantly excited satellite spectral components (Fig. 8, bottom).

Under near-optimum resonant excitation in the $I^*_{2c,d}$ PLE feature, the I^{In*}_{2s} satellite falls very close in energy to the I^{Cl}_3 line (compare upper and lower PL spectra in Fig. 8). This is the reason for the appearance of the very sharp components I^{In*}_{2s} and I^{In*}_{2p} in the PLE spectrum of I^{Cl}_3 luminescence [Fig. 9(b)]. These components have nothing to do with the I^{Cl}_3 transition. However, there is a weak component near 2.815_5 eV which may represent an excited state of an exciton bound to an *ionized* donor associated with the $n=2$ FE. Similarly the additional component between I^*_{20} and $I^*_{2c,d}$ labeled I^{0*}_α in Fig. 2, enhanced for detection of I^{LO}_α luminescence, may be attributed to such a BE excited state for the center responsible for I^0_α. It is not possible to decide whether a further special excited BE component associated with I^{DEEP}_1 may occur in this region, since it would fall close to the strong phonon replica $I^{DEEP\ LO}_1$ (Fig. 10).

The intensity ratio between I^{In*}_{2s} and I^{In*}_{2p}, about 20:1 according to the lower spectrum in Fig. 8, is very much larger even than the two-electron satellites of the principal DBE lines, about 4:1 for the In donor and only ~1.2:1 for the Cl donor. These intensity ratios provide information about the character of the excited DBE states. For example, two-electron satellites of the excited DBE states such as I_{2_b} exhibit a very small value of this ratio, ~0.03, similar to the values for analogous transitions in ZnTe.[10] This has been shown to confirm earlier theoretical suggestions[8] that the main excited DBE states in this region involve hole excitations to p-like orbital states, assuming that strong electron-hole correlation exists for these very weakly bound excitons. Analogous arguments suggest that the character of the $I^*_{2c,d}$ DBE excited states is quite different. These states involve qualitatively different types of internal excitations within the DBE complex. Excited states such as I_{2_b} are associated with excitations of the electron-hole pair as an entity within the field of the neutral donor. The lowest-lying available excited states involve p-like wave functions of the bound hole, as already discussed. The $I^*_{2c,d}$ states involve excitations within the bound electron-hole pair, in which the electron is placed in an orbital state relative to the hole similar to the $n=2$ state of the FE. Transitions to the $2s_{3/2}$ state of the FE should predominate in one-photon absorption processes. Let the DBE wave function Ψ_{BE} be approximated by the product form

$$\Psi_{BE} \approx \psi_D(r)\Phi(R)\psi_{FE}(r-R)\ , \tag{3}$$

where $\psi_D(r)$ is the electron wave function of the $1s$ donor ground state, $\psi_{FE}(r-R)$ is the wave function of the FE ns state centered on position R, approximately the position of the bound hole since $m^*_e/m^*_h \ll 1$, and $\Phi(R)$ represents the envelope state of the quasi-FE orbiting about the neutral donor.

Since both ψ_{FE} and ψ_D involve s states, then strong transitions to p-like DBE states will occur only if $\Phi(R)$ is p-like. We therefore conclude that $I^*_{2c,d}$ has s-like envelope character. Resonant excitation into I^*_{20} near 2.814_1 eV shows I^{Cl*}_{2p} to be dominant (Fig. 8), so we conclude that this excited DBE state has a dominant p-like envelope. Unfortunately, two-electron satellites involving the In donor fall within the ABE components $I^{Li,Na}_1$ under resonant excitation within I^*_{20}, and it is difficult to establish a value for the ratio $I^{In*}_{2s}/I^{In*}_{2p}$ in this SPL.

The apparent splitting of $I^*_{2c,d}$ in a magnetic field [Fig. 9(a)] may arise from a separation of the initially degenerate BE excited states involving different donors and also possibly, different excited states of the FE. For example, a $3s$ excited quasi-FE state bound with a p-like envelope function $\Phi(R)$ could fall near $I^*_{2c,d}$, 2.5 meV above I^*_{20}, the component associated with a $2p$-like state of $\Phi(R)$. Calculations by Baldereschi and Lipari[29] suggest that the 4 $2p$-like and single $2s$-like FE excited states all lie within a range of binding energy from 4.9 to 6.2 meV for ZnSe. Thus, there is ample scope for contributions $I^*_{2c,d}$ from a variety of $n=2$ quasi-FE states, with energy transfer from s to p states by absorption processes involving the emission of appropriate low-energy acoustic phonons.

Finally, we note that the small value of the intensity ratio $I^{In*}_{2s}/I^{In*}_{2p}$ ~0.1 observed in the PLE spectrum of Fig. 9(b) does not conflict with the evidence in Fig. 8 that this ratio is large; ~20:1. The point is that the overlap of the excitation energy with the portion of the broad $I^*_{2c,d}$ excited-state absorption band relevent for In donors, on the high-energy side according to the above discussion, is much better for the $1s \rightarrow 2p$ excitation energy of the In donor, measured relative to the 2.7960 eV detected energy than it is for the $1s-2s$ excitation energy. The strength of the I^{In*}_{2p} PLE feature decreased rapidly with increasing magnetic field [Fig. 9(b)]. Much of this decrease is due to the large orbital splitting of the $2p$ state. Only two-electron transitions

to the $2p_0$ magnetic subcomponent can produce luminescence detectable in this experiment because of the precise match required for the sum of the detected energy and the satellite displacement energy with the excited DBE absorption band. The residual intensity decrease above $B \sim 3\,T$ is presumably due to decreasing overlap arising from the differential diamagnetic shift between the $2p_0$ excited-state donor energy and the $I^{In*}_{2c,d}$ PLE band.

ACKNOWLEDGMENTS

The authors are grateful to J. L. Merz (Bell Laboratories) for the VG ZnSe crystals used in this work and to Diana Beardsley and P. Porteous, S. P. Herko, and T. McGee for experimental assistance. Special thanks are due to J. R. Hughes and particularly to A. M. White for programming calculator control of the spectrometer.

[1]L. S. Pedrotti and D. C. Reynolds, Phys. Rev. 120, 1664 (1960).
[2]D. G. Thomas and J. J. Hopfield, Phys. Rev. 128, 2135 (1962).
[3]Discussed in Sec. 3.2.2 of *Excitons*, edited by K. Cho, Topics in Current Physics (Springer, Berlin, 1979), Vol. 14, p. 67.
[4]J. J. Hopfield, *Proceedings of the International Conference on the Physics of Semiconductors, Paris, 1964* (Dunod, Paris, 1964), p. 725.
[5]J. L. Merz, H. Kukimoto, K. Nassau, and J. W. Shiever, Phys. Rev. B 6, 545 (1972).
[6]H. Venghaus and P. J. Dean, Phys. Rev. B 21, 1596 (1980).
[7]H. Tews and H. Venghaus, Solid State Commun. 30, 219 (1979).
[8]D. C. Herbert, J. Phys. C 10, 3327 (1977).
[9]R. Romestain and N. Magnea, Solid State Commun. 32, 1201 (1979).
[10]P. J. Dean, D. C. Herbert, and A. M. Lahee, J. Phys. C, in press.
[11]K. Kosai, B. J. Fitzpatrick, H. G. Grimmeiss, R. N. Bhargava, and G. F. Neumark, Appl. Phys. Lett. 35, 194 (1979).
[12]R. N. Bhargava, R. J. Seymour, B. J. Fitzpatrick, and S. P. Herko, Phys. Rev. B 20, 2407 (1979).
[13]K. Nassau and J. W. Shiever, J. Cryst. Growth 13-14, 375 (1972).
[14]C. J. Werkhoven, R. N. Bhargava, B. J. Fitzpatrick, S. P. Herko, and P. J. Dean, Bull. Am. Phys. Soc. 25, 204 (1980). [The preliminary view reported here that this new bound exciton with localization energy ~3.8 meV (4.5 meV according to the exciton band gap of 2.8027 eV used in this paper), involves a new donor species has been found incorrect on closer examination].
[15]C. J. Werkhoven, B. J. Fitzpatrick, S. P. Herko, R. N. Bhargava, and P. J. Dean, Appl. Phys. Lett. 38, 540 (1981).
[16]P. J. Dean, Czech. J. Phys. B 30, 272 (1980).
[17]D. J. Dunstan, J. E. Nicholls, B. C. Cavenett, J. J. Davies, and K. V. Reddy, Solid State Commun. 24, 677 (1977).
[18]For example, the case of the Bi isoelectronic trap in GaP; P. J. Dean and R. A. Faulkner, Phys. Rev. 185, 1064 (1969).
[19]M. Lax, Phys. Rev. 119, 1502 (1960).
[20]H. B. De Vore, Phys. Rev. 102, 86 (1956).
[21]P. J. Dean, Phys. Rev. 168, 889 (1968).
[22]J. Conradi and R. R. Haering, Phys. Rev. 185, 1088 (1969).
[23]R. Ulbrich, Phys. Rev. B 8, 5719 (1973).
[24]H. Venghaus and R. Lambrich, Solid State Commun. 25, 109 (1978).
[25]H. Venghaus, Phys. Rev. B 19, 3071 (1979).
[26]A. Baldereschi and N. O. Lipari, Phys. Rev. B 8, 2697 (1973).
[27]M. Sondergeld and R. G. Stafford, Phys. Rev. Lett. 35, 1529 (1975).
[28]P. J. Dean, J. Lumin. 21, 75 (1979).
[30]A. Baldereschi and N. O. Lipari, Phys. Rev. B 3, 439 (1971).